Effect of Charge Localization on the Effective Hyperfine Interaction in Organic Semiconducting Polymers

Rugang Geng,[1] Ram C. Subedi,[1] Hoang M. Luong,[1] Minh T. Pham,[1] Weichuan Huang,[2] Xiaoguang Li,[2] Kunlun Hong,[3] Ming Shao,[3] Kai Xiao,[3] Lawrence A. Hornak,[4] and Tho D. Nguyen[1,*]

[1]*Department of Physics and Astronomy, University of Georgia, Athens, Georgia 30602, USA*

[2]*Hefei National Laboratory for Physical Sciences at the Microscale, Department of Physics, and Collaborative Innovation Center of Advanced Microstructures, University of Science and Technology of China, Hefei 230026, China*

[3]*Center for Nanophase Materials Sciences, Oak Ridge National Laboratory, Oak Ridge, Tennessee 37831, USA*

[4]*College of Engineering, University of Georgia, Athens, Georgia 30602, USA*

(Received 1 September 2017; revised manuscript received 10 February 2018; published 22 February 2018)

Hyperfine interaction (HFI), originating from the coupling between spins of charge carriers and nuclei, has been demonstrated to strongly influence the spin dynamics of localized charges in organic semiconductors. Nevertheless, the role of charge localization on the HFI strength in organic thin films has not yet been experimentally investigated. In this study, the statistical relation hypothesis that the effective HFI of holes in regioregular poly(3-hexylthiophene) (P3HT) is proportional to $1/N^{0.5}$ has been examined, where N is the number of the random nuclear spins within the envelope of the hole wave function. First, by studying magnetoconductance in hole-only devices made by isotope-labeled P3HT we verify that HFI is indeed the dominant spin interaction in P3HT. Second, assuming that holes delocalize fully over the P3HT polycrystalline domain, the strength of HFI is experimentally demonstrated to be proportional to $1/N^{0.52}$ in excellent agreement with the statistical relation. Third, the HFI of electrons in P3HT is about 3 times stronger than that of holes due to the stronger localization of the electrons. Finally, the effective HFI in organic light emitting diodes is found to be a superposition of effective electron and hole HFI. Such a statistical relation may be generally applied to other semiconducting polymers. This Letter may provide great benefits for organic optoelectronics, chemical reaction kinetics, and magnetoreception in biology.

DOI: 10.1103/PhysRevLett.120.086602

Organic semiconductors (OSECs) are characterized by weak spin-orbit coupling (SOC) and small HFI, which are associated with π-orbital electrons in a lightweight element environment. This makes them attractive candidates for spintronic devices [1,2]. On one hand, the weak spin interaction in OSECs results in a long spin lifetime in comparison to their inorganic couterparts [3]. The long spin lifetime makes them promising candidates for obtaining large magnetoresistance (MR) in organic spin valves (OSVs) [4], and coherent spin manipulation in logic devices such as spin transistors [5]. On the other hand, SOC and HFI are important ingredients of spin mixing mechanisms in OSECs, originating organic magnetoresistance (OMAR) in organic light emitting diodes (OLEDs) [6–17]. Generally, OMAR in OLEDs may be considered as a much broader research field that deals with magnetic-field effects (MFE) in physics [6], chemistry [18], and biology [19]. Properties such as optoelectronics, chemical reaction kinetics, and magnetoreception are believed to be governed by HFI and/or SOC, and external magnetic fields. Some HFI- and SOC-based mechanisms have been proposed to explain OMAR. In the electron-hole (or polaron) pair mechanism, HFI and SOC are believed to govern the singlet-triplet interconversion rate, and therefore affect the optoelectronic property of the material [14]. In the bipolaron mechanism, HFI influences the hopping mobility of charges and hence affects the electrical property of the material [8,9]. Several other mechanisms such as Δg, triplet-triplet annihilation, and charge-exciton scattering mechanisms have also been widely discussed in the literature; however, such mechanisms do not directly rely on HFI and SOC [10–12].

Although SOC and HFI in OSECs have been extensively studied for the past decade, it is challenging to identify the dominant spin loss mechanism in OSECs. For example, the detection of the pure spin current in conventional OSECs by using the inverse spin Hall effect technique is the most obvious evidence for the existence of SOC in the materials [20–23]. Nevertheless, such experiments do not answer the question regarding the dominant spin loss mechanism in conventional OSECs. Recently, Nguyen *et al.* [15] and Malissa *et al.* [17] reported that the main spin related interaction in poly(p-phenylene vinylene) (PPV)-based polymers has been attributed to HFI. Despite the domination of HFI in PPV polymers, several studies showed that the effective spin related interaction significantly depends on fabrication conditions [11,16] and electrical conditioning

[13] that directly affect charge localization. Such unknown variation complicates the ability to distinguish between HFI and SOC in conventional OSECs. A better understanding of the origin of HFI strength would benefit not only the field of organic spintronics, but also the research of spin in organics.

In semiconductors, the localized electron spin interacts with a large number (N) of unpolarized quasistationary nuclear spins that are localized inside the envelope of the electron's wave function. Statistically, the effective fluctuating magnetic field, a_{HFI} (also known as the Overhauser field, and HFI constant), caused by N random nuclear spins can be described as $a_{\mathrm{HFI}} \sim A_{\mathrm{HFI}}/N^{0.5}$, where A_{HFI} is the field caused by an individual nuclear spin [24]. This collective behavior has been optically and electrically evaluated in quantum dots made by inorganic semiconductors where the electron confinement depends on the dot's size [24–26]. However, such an important statistical origin of HFI strength has not been investigated in solid state OSECs. Such a statistical relation is analogous to the McConnell equation, which successfully describes the proportional dependence of a_{HFI} on the unpaired electron spin density in aromatic radical compound solutions [27]. Recent electron paramagnetic resonance (EPR) studies of oligomers also in solution show that a_{HFI} decreases with increasing the number of repeat units due to the extensive charge delocalization on the isolated oligomer chains [28–31]. The HFI, which is typically in the order of 10 G, however, might be seriously quenched in such magnetic resonance technique at 3 kG [32]. In addition, since the electronic properties of oligomers strongly depend on the chain length, it is challenging to use such oligomers in devices to test the statistical origin of HFI.

In this Letter, we investigate the statistical origin of HFI in P3HT polymers using hole-only devices. The localization length of holes (or positive polarons) in P3HT has been theoretically calculated up to 15 thiophene units (~6 nm) [33]. By assuming that holes delocalize fully over the P3HT polycrystalline domain, and considering the first and second nearest hydrogens neighboring the backbone chain, N ranges from 100 to 1000, which is a good statistical ensemble to test the hypothesis, and it can be largely tuned by thermal annealing. We also investigate the relationship between effective HFIs of electrons, holes, and electron-hole pairs in several semiconducting polymers.

Several π-conjugated polymers, either synthesized in house or purchased from commercial sources, were used in this study. We synthesized two isotope-labeled polymers: regioregular hydrogenated P3HT and full deuterated P3HT (Hereafter FD-P3HT). In FD-P3HT, all hydrogen atoms (^{1}H, nuclear spin $I = \frac{1}{2}$) were replaced by deuterium atoms [^{2}H (D), $I = 1$], which have a much smaller HFI constant a, namely, $a(\mathrm{D}) = a(\mathrm{H})/6.5$. The inset of Fig. 1(a) shows the isotope-labeled P3HT structures, and the synthesis process can be found elsewhere [34]. To ensure that all the hydrogen atoms are replaced by deuterium atoms in FD-P3HT, we performed Raman scattering spectra [Fig. 1(a)].

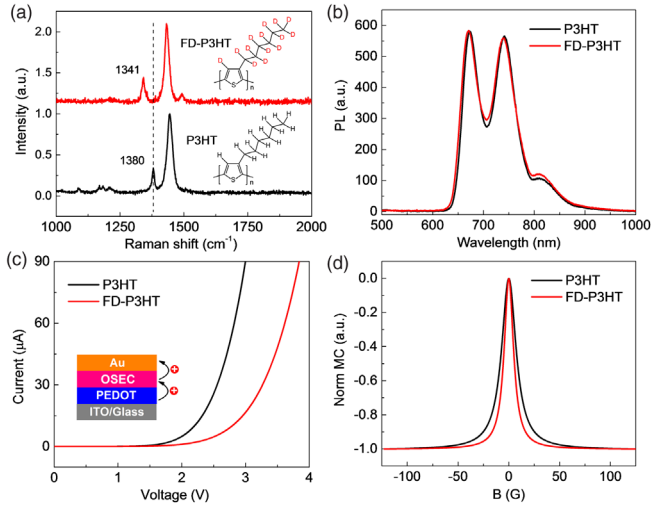

FIG. 1. (a) Raman spectra of isotope-labeled P3HT. The insets show the chemical structures of hydrogenated P3HT and full-deuterated P3HT. (b) Photoluminescence of the isotopes at a low temperature of 10 K. (c) IV characteristics and (d) MC (with 0.5 G resolution) of the isotope-based hole-only devices at 10 K.

It is seen that the two main Raman-active vibrational modes at 1380 cm^{-1} (CH—CH stretching) and 1446 cm^{-1} (CH═CH stretching) are redshifted by about 3% and 1%, respectively upon deuteration; this is in agreement with the expected isotope shift in the CH (CD) units due to the "square root of the mass ratio rule." Figure 1(b) shows that the photoluminescence (PL) spectra of the P3HT and FD-P3HT thin films are essentially the same, thus verifying that the polymer electronic structures are the same in the homemade P3HT polymers. The x-ray diffraction (XRD) spectra of annealed films confirm that the synthesized materials have a similar semicrystalline structure [Fig. S1(c) in the Supplemental Material [35]]. Figure 1(c) shows the current-voltage (I-V) characteristics of two hole-only devices made by the isotope-labeled P3HT. The slight difference on the conductivity is due to the slight difference in device thickness. Figure 1(d) shows that the magnetoconductivity (MC) of the devices measured at 10 K with a current density of ~50 μA/mm^2 is saturated at 125 G applied field. The figure clearly shows that P3HT has the half width at half maximum (HWHM) of 8.6 G, much larger than the HWHM of 5.6 G in FD-P3HT. Our result has a similar OMAR width ratio in PPV-based isotopes [14,21]. The result clearly proves that HFI is dominant in P3HT at small applied field range. We note that such isotope study itself can not exclude the existence of SOC [39], but SOC might only have a non-negligible effect on OMAR at above ~100 mT [40]. In addition, gas chromatography-mass spectroscopy and nuclear magnetic resonance measurements show that the deuteration level of FD-P3HT was about 97%–98%, which might be another factor to reduce the HFI difference.

We are now in the position to evaluate the statistical origin of HFI, where the polycrystalline domain size is

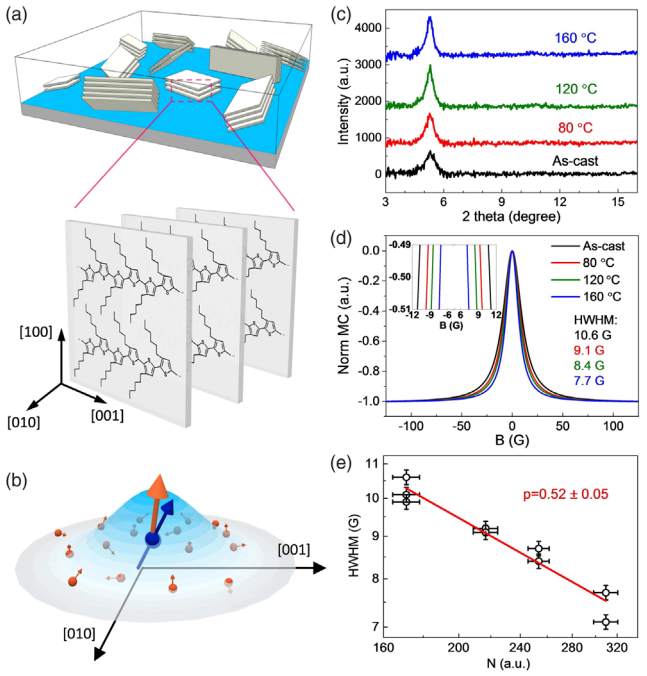

FIG. 2. (a) A cartoon of the P3HT as-cast thin film where the crystalline domains are mixed with the amorphous states, and the inset shows the crystallographic directions. [010] is the π–π stacking direction. (b) The spatial distribution of electron wave function in the lamellar (100) plane. The small orange arrows represent the hydrogen nuclear spins that generate an effective hyperfine field B_{HFI} (large orange arrow) at the electron spin (blue arrow). (c) XRD spectra of annealed and as-cast films made by commercial P3HT. (d) MC (with 0.5 G resolution) of the hole-only devices corresponding to annealed and as-cast P3HT films at 10 K. (e) MC HWHM of the commercial P3HT hole-only devices versus the number of nuclear spins at 10 K (in log-log scale). The line shows a fit with the $1/N^{p}$ function. The current density in (d) and (e) is $\sim$50 μA/mm^2.

crucial for estimating number N. It has been widely studied that thin P3HT films prepared by solution spin-casting contain randomly oriented polycrystalline and amorphous domains [41]. Film annealing usually leads to an increase in the crystal coherence length or domain size. The cause of this is a higher degree of head-to-tail regioregularity, stronger π–π interchain interactions and a reduction of the torsional angle between the monomers. Consequently, this reduces the conjugated break possibility in the material leading to better charge delocalization. With film annealing, we observed the growth of the crystallite caused by the phase transition from amorphous domains into semicrystalline domains. This can be seen in Fig. 2(c) where the width of the XRD diffraction peak of the annealed P3HT film becomes narrower when increasing the annealing temperature. Using Scherrer's equation, we estimate that the average domain size in the films varies from 13.1 to 17.6 nm (Fig. S3 and Table S1 in the Supplemental Material [35]). These sizes are a few times larger than the reported hole localization length in the materials [33].

Figure 2(d) shows the MC response of hole-only devices made by commercial P3HT at 10 K in the field range of 125 G at different annealing conditions. Upon increasing the annealing temperature, the HWHM of MC gradually reduces from $\sim$10.6 to $\sim$7.0 G while the MC magnitude generally decreases (Fig. S4 in the Supplemental Material [35]). There are several important results associated with the MC width dynamics. First, the reduction of MC width was consistently observed at all temperatures (Fig. S5 in the Supplemental Material [35]) and with different current densities (Fig. S6 in the Supplemental Material [35]). Second, the MC width is essentially independent of the current density and the hopping rate (Fig. S7 in the Supplemental Material [35]), which indicates that the narrowing of the MC width is not caused by the change of the hopping rate as proposed in the bipolaron model [8,9]. Finally, the MC width broadening cannot originate from the Δg spin mixing mechanism since only one type of carrier exists in the unipolar devices [12]. Our result indicates that the reduction of the MC width is caused by the reduction of the effective HFI of holes in the semicrystalline P3HT film and the latter is due to the growth of the domain size upon annealing. The conclusion agrees with the recent density functional theory (DFT) calculation, in which the HFI strength, rather than SOC strength strongly depends on the localization length of holes in the P3HT polymer [33]. Similar reduction of the MC width in the homemade P3HT polymers has been observed as well (Fig. S8 in the Supplemental Material [35]).

To quantitatively estimate the density of the hydrogen nuclei within the localization length of holes in annealed films relative to the as-cast films, we assume that the hole localization length in the lamellar plane is proportional to the effective microcrystalline size, which can be estimated from XRD spectroscopy. This assumption is generally correct in inorganic semiconductors since the delocalization length of the electron wave function in bulk material is normally larger than that the dot's size [42]. Such a condition might be correctly applied to holes in the P3HT domain where the calculated delocalization length in one dimension of 6 nm is reported [33]. The extension of the hole wave function in semicrystalline P3HT is preferably in the 2D lamellar plane that might essentially exceed the domain size. Assuming the nuclear spins distributed uniformly, the effective HFI strength in the P3HT film can be appropriately written as $a_{\mathrm{HFI}} \propto 1/N^{0.5} \propto 1/d$, where d is the average domain size in the films at different annealing conditions. Figure 2(e) shows that the larger the N ($\propto d^2$), the smaller the MC HWHM or HFI strength. The solid line shows the best fit of HFI strength, $a_{\mathrm{HFI}} \propto 1/N^{p}$, where $p = 0.52 \pm 0.05$. This result excellently agrees with the statistical relation, where p is equal to 0.5.

To further verify the HFI strength in P3HT films, one of the most effective ways is to measure the spin diffusion length of P3HT films in OSVs where the P3HT film is sandwiched

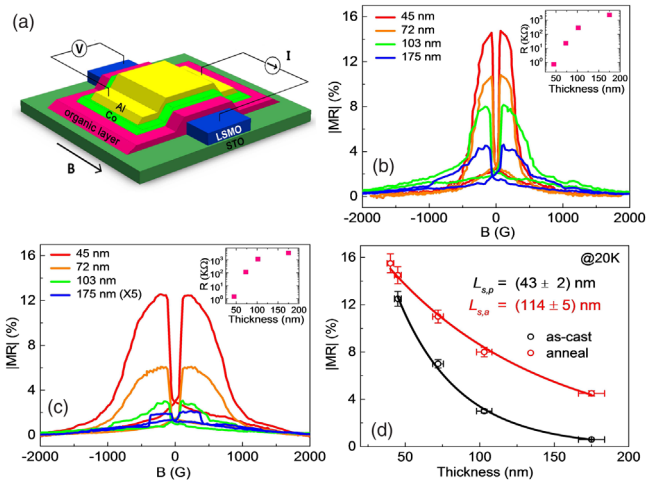

FIG. 3. (a) Schematic representation of the organic spin valve (OSV) with four probe measurement. MR response at 20 K of OSVs (b) with film annealing at 160 °C and (c) without film annealing at different P3HT thicknesses. (d) Thickness-dependent MR magnitude (dots) at 20 K. The solid lines show fits using the modified Jullière model.

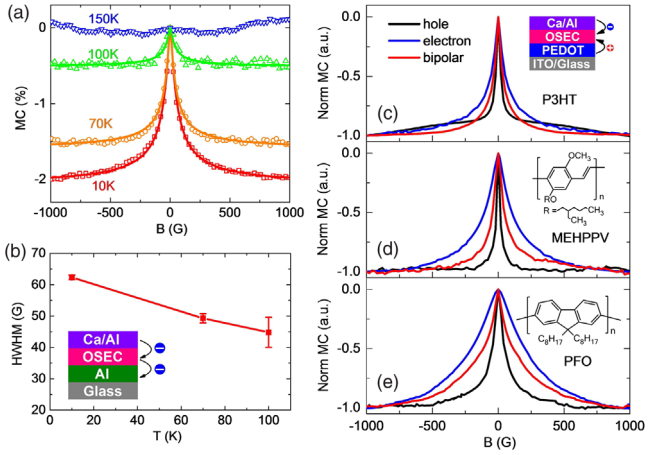

FIG. 4. MC responses of an electron-only device (a) at different temperatures, and (b) their MC HWHM. Normalized MC responses of hole-only, electron-only, and bipolar devices made by (c) P3HT, (d) MEH-PPV, and (e) PFO. All MCs were measured with the current density of 10 μA/mm^2 and field resolution of 5 G.

between two ferromagnetic electrodes of $La_{2/3}Sr_{1/3}MnO_3$ (LSMO) and Co [Fig. 3(a)] [4]. According to the modified Jullière model, the magnitude of MR is given by [43]

$$\left(\frac{\Delta R}{R}\right)_{\max} = \frac{2P_1P_2e^{-d/L_s}}{1-P_1P_2e^{-d/L_s}}, \tag{1}$$

where P_1 and P_2 are the effective spin polarizations at the interface of the ferromagnetic electrodes (dubbed spinterface), L_s is the spin diffusion length of the spacer, and d is the thickness of the spacer. Figure 3(b) [3(c)] shows the MR responses with different thicknesses made by annealed (as-cast) P3HT films at 20 K with junction voltage of −20 mV. The corresponding resistance of the devices at −20 mV is shown in their insets. Figure 3(d) shows the fit of the thickness dependent MR using Eq. (1), which yields the spin diffusion length of the annealed film, $L_{s,a} = (114 \pm 5)$ nm and the spin diffusion length of the as-cast film, $L_{s,p} = (43 \pm 2)$ nm at 20 K. The spinterface product P_1P_2 of the electrodes is 0.08 and 0.12 for annealed and as-cast devices at 20 K, respectively, which indicates that the film annealing may also significantly modify the spinterface of the ferromagnetic electrodes [4,44]. Our MR result is in good agreement with the MR results reported by Majumdar *et al.* [45] and Morley *et al.* [46] To estimate the relative HFI strengths of two films from spin diffusion length, we employ the numerical results from Bobbert *et al.* [47]. At a certain limit, the spin diffusion length can be written as $L_s = (r^2/2)t$, where t is the intermolecular distance and r is the ratio of the spin-precession period (caused by the hyperfine field) to the average time that the carrier spends on each hopping site. In P3HT film, the charge is localized in the lamellar plane, which is predominantly oriented parallel to the substrate [41]. Therefore, the transport that happens perpendicular to the lamellar plane would have very similar hopping distances in both annealed and as-cast films [41]. Since the resistance of the OSVs with the same thickness is similar [insets in Fig. 3(b) and 3(c)], the average dwell time on each hopping site of a hole would be similar. In the first order approximation, we can estimate that the HFI strength ratio between the annealed ($a_{\mathrm{HFI},a}$) and as-cast ($a_{\mathrm{HFI},p}$) films is $(a_{\mathrm{HFI},a}/a_{\mathrm{HFI},p}) \approx \sqrt{(L_{s,p}/L_{s,a})} \approx 0.61$. This is in excellent agreement with the effective HFI ratio $(a_{\mathrm{HFI},a}/a_{\mathrm{HFI},p}) \approx 0.70$ achieved by the OMAR response as shown in Fig. 2(e).

The other effective way to qualitatively examine the statistical origin of the effective HFI strength in OSECs is to compare the localization of electrons and holes in the same material in which they experience the same nuclear spin ensemble. Figure 4(a) shows the temperature dependent MC response of an electron-only device made by as-cast commercial P3HT at the 1000 G field range. The HWHM of the MC is shown in Fig. 4(b). Interestingly, we observed the HWHM decrease from 62 G at 10 K to ~45 G at 100 K. The HWHM in the electron-only device is about 3 times larger than that in the hole-only device (Table S2 in the Supplemental Material [35]). We can conclude that the HFI of electrons is about 3 times stronger than the HFI of holes, in agreement with that in PPV-based polymers [48]. The larger HFI of electrons is attributed to their stronger localization. We speculate that if the hole mobility is larger than the electron mobility in a semiconducting polymer, the hole should have smaller HFI than the electron. Figures 4(c), 4(d), and 4(e) show the normalized MC responses of electron-only (blue lines) and hole-only devices (black lines) made by P3HT, MEH-PPV (Poly[2-methoxy-5-(2-ethylhexyloxy)-1,4-phenylenevinylene]) and PFO (polyfluorene) at 10 K in the field range of 1000 G.

Because of the large scanning field step, the MC width of P3HT in Fig. 4(c) is slightly broader than that in Fig. 2(d). Similar to P3HT, Figs. 4(d) and 4(e) show that the hole HFI is significantly smaller than the electron HFI in the p-type MEH-PPV and PFO polymers (Table S2 in the Supplemental Material [35]) [49]. Generally, the comparison of HFI on charge mobility between different polymers is not possible since the charge mobility depends on the energetic and positional disorders, which strongly depend on the polymer structure and composition.

We finally show studies of the OMAR effect in bipolar devices or OLEDs. We found that effective HFI in OLEDs is a superposition of electron and hole HFIs in the same polymer. As a result, the effective HFI in OLEDs would be affected by the electron and hole localizations. Figures 4(c),4(d), and 4(e) show the normalized OMAR response (pink lines) in OLEDs made with three different polymers at 10 K. The effective HFI in OLEDs is smaller than the average of electron and hole HFIs (Fig. S10 and Table S2 in the Supplemental Material [35]). This is because the extension of the wave function of electrons and holes in bipolar devices may be slightly larger than that in homopolar devices due to their charge neutrality. In addition, the OMAR effect in OLEDs at large field might also be influenced by some other mechanisms, such as triplet-triplet annihilation and charge-exciton scattering [10,11]. We note that the empirical formula found by Weller *et al.* [50] for calculating the effective HFI in radical ion-pair solutions cannot be used to estimate the effective HFI in OLEDs. The reason might belong to the stronger charge localization in the isolated molecules.

In conclusion, we have demonstrated the statistical origin of HFI strength of holes in P3HT polymers. The HFI strength was found to be inversely proportional to the localization length of holes. We also found that electrons have a much larger HFI than holes due to electrons' stronger localization. Finally, the effective HFI in OLEDs made by several polymers is a superposition of the effective electron and hole HFIs.

We acknowledge the useful discussion with Professor Valy Vardeny, Professor Eitan Ehrenfreund, Professor Manh-Huong Phan, and Dr. Andreas Sperlich. We thank Professor Yiping Zhao group for helping us with the XRD measurement. Synthesis of the isotope-labeled P3HT and the corresponding Raman and XRD measurement were conducted at the Center for Nanophase Materials Sciences, which is a DOE Office of Science User Facility. This work was supported by the University of Georgia (UGA) startup funds and Faculty Research Grant (T. D. N.), startup funds provided by the UGA College of Engineering (L. A. H), NSFC, and National Key Research and Development Program of China (Contracts No. 2016YFA0300103 and No. 2015CB921201, X. L.).

*ngtho@uga.edu

[1] V. A. Dediu, L. E. Hueso, I. Bergenti, and C. Taliani, Nat. Mater. **8**, 707 (2009).
[2] S. Sanvito, Chem. Soc. Rev. **40**, 3336 (2011).
[3] S. Sanvito, Nat. Mater. **6**, 803 (2007).
[4] J. Devkota, R. Geng, R. C. Subedi, and T. D. Nguyen, Adv. Funct. Mater. **26**, 3881 (2016).
[5] S. Datta and B. Das, Appl. Phys. Lett. **56**, 665 (1990).
[6] R. Geng, T. T. Daugherty, K. Do, H. M. Luong, and T. D. Nguyen, J. Sci. Adv. Mater. Devices **1**, 128 (2016).
[7] Y. Sheng, D. T. Nguyen, G. Veeraraghavan, O. Mermer, M. Wohlgenannt, S. Qiu, and U. Scherf, Phys. Rev. B **74**, 045213 (2006).
[8] P. A. Bobbert, T. D. Nguyen, F. W. A. van Oost, B. Koopmans, and M. Wohlgenannt, Phys. Rev. Lett. **99**, 216801 (2007).
[9] F. L. Bloom, W. Wagemans, M. Kemerink, and B. Koopmans, Phys. Rev. Lett. **99**, 257201 (2007).
[10] P. Desai, P. Shakya, T. Kreouzis, and W. P. Gillin, J. Appl. Phys. **102**, 073710 (2007).
[11] B. Hu and Y. Wu, Nat. Mater. **6**, 985 (2007).
[12] F. J. Wang, H. Bässler, and Z. Valy Vardeny, Phys. Rev. Lett. **101**, 236805 (2008).
[13] U. Niedermeier, M. Vieth, R. Pätzold, W. Sarfert, and H. von Seggern, Appl. Phys. Lett. **92**, 193309 (2008).
[14] T. D. Nguyen, G. Hukic-Markosian, F. Wang, L. Wojcik, X.-G. Li, E. Ehrenfreund, and Z. V. Vardeny, Nat. Mater. **9**, 345 (2010).
[15] T. D. Nguyen, B. R. Gautam, E. Ehrenfreund, and Z. V. Vardeny, Phys. Rev. Lett. **105**, 166804 (2010).
[16] J. Rybicki, R. Lin, F. Wang, M. Wohlgenannt, C. He, T. Sanders, and Y. Suzuki, Phys. Rev. Lett. **109**, 076603 (2012).
[17] H. Malissa, M. Kavand, D. P. Waters, K. J. van Schooten, P. L. Burn, Z. V. Vardeny, B. Saam, J. M. Lupton, and C. Boehme, Science **345**, 1487 (2014).
[18] U. E. Steiner and T. Ulrich, Chem. Rev. **89**, 51 (1989).
[19] K. Maeda, K. B. Henbest, F. Cintolesi, I. Kuprov, C. T. Rodgers, P. A. Liddell, D. Gust, C. R. Timmel, and P. J. Hore, Nature (London) **453**, 387 (2008).
[20] S. Watanabe, K. Ando, K. Kang, S. Mooser, Y. Vaynzof, H. Kurebayashi, E. Saitoh, and H. Sirringhaus, Nat. Phys. **10**, 308 (2014).
[21] D. Sun, K. J. van Schooten, M. Kavand, H. Malissa, C. Zhang, M. Groesbeck, C. Boehme, and Z. Valy Vardeny, Nat. Mater. **15**, 863 (2016).
[22] J. B. S. Mendes, O. Alves Santos, J. P. Gomes, H. S. Assis, J. F. Felix, R. L. Rodríguez-Suárez, S. M. Rezende, and A. Azevedo, Phys. Rev. B **95**, 014413 (2017).
[23] R. Das, V. Kalappattil, R. Geng, H. Luong, M. Pham, T. Nguyen, T. Liu, M. Wu, M. H. Phan, and H. Srikanth, AIP Adv. **8**, 055906 (2018).
[24] A. C. Johnson, J. R. Petta, J. M. Taylor, A. Yacoby, M. D. Lukin, C. M. Marcus, M. P. Hanson, and A. C. Gossard, Nature (London) **435**, 925 (2005).
[25] A. S. Bracker, E. A. Stinaff, D. Gammon, M. E. Ware, J. G. Tischler, A. Shabaev, A. L. Efros, D. Park, D. Gershoni, V. L. Korenev, and I. A. Merkulov, Phys. Rev. Lett. **94**, 047402 (2005).
[26] J. Hansom, C. H. H. Schulte, C. Le Gall, C. Matthiesen, E. Clarke, M. Hugues, J. M. Taylor, and M. Atature, Nat. Phys. **10**, 725 (2014).
[27] H. M. McConnell, J. Chem. Phys. **24**, 764 (1956).
[28] A. A. Zezin, V. I. Feldman, J. M. Warman, J. Wildeman, and G. Hadziioannou, Chem. Phys. Lett. **389**, 108 (2004).

[29] K. Susumu, P. R. Frail, P. J. Angiolillo, and M. J. Therien, J. Am. Chem. Soc. **128**, 8380 (2006).
[30] J. Rawson, P. J. Angiolillo, and M. J. Therien, Proc. Natl. Acad. Sci. U.S.A. **112**, 13779 (2015).
[31] M. D. Peeks, C. E. Tait, P. Neuhaus, G. M. Fischer, M. Hoffmann, R. Haver, A. Cnossen, J. R. Harmer, C. R. Timmel, and H. L. Anderson, J. Am. Chem. Soc. **139**, 10461 (2017).
[32] B. Koopmans, Nat. Phys. **10**, 249 (2014).
[33] J. Niklas, K. L. Mardis, B. P. Banks, G. M. Grooms, A. Sperlich, V. Dyakonov, S. Beaupre, M. Leclerc, T. Xu, L. Yu, and O. G. Poluektov, Phys. Chem. Chem. Phys. **15**, 9562 (2013).
[34] M. Shao, J. Keum, J. Chen, Y. He, W. Chen, J. F. Browning, J. Jakowski, B. G. Sumpter, I. N. Ivanov, Y.-Z. Ma, C. M. Rouleau, S. C. Smith, D. B. Geohegan, K. Hong, and K. Xiao, Nat. Commun. **5**, 3180 (2014).
[35] See Supplemental Material at http://link.aps.org/supplemental/10.1103/PhysRevLett.120.086602 for XRD characterization of P3HT films, device fabrication and measurement, and the MC measurements in detail, which includes Refs. [36–38].
[36] B. K. Crone, I. H. Campbell, P. S. Davids, and D. L. Smith, Appl. Phys. Lett. **73**, 3162 (1998).
[37] A. J. Campbell, D. D. C. Bradley, T. Virgili, D. G. Lidzey, and H. Antoniadis, Appl. Phys. Lett. **79**, 3872 (2001).
[38] C. Waldauf, M. Morana, P. Denk, P. Schilinsky, K. Coakley, S. A. Choulis, and C. J. Brabec, Appl. Phys. Lett. **89**, 233517 (2006).
[39] L. Nuccio *et al.*, Phys. Rev. Lett. **110**, 216602 (2013).
[40] G. Joshi, R. Miller, L. Ogden, M. Kavand, S. Jamali, K. Ambal, S. Venkatesh, D. Schurig, H. Malissa, J. M. Lupton, and C. Boehme, Appl. Phys. Lett. **109**, 103303 (2016).
[41] E. Verploegen, R. Mondal, C. J. Bettinger, S. Sok, M. F. Toney, and Z. Bao, Adv. Funct. Mater. **20**, 3519 (2010).
[42] R. Hanson, L. P. Kouwenhoven, J. R. Petta, S. Tarucha, and L. M. K. Vandersypen, Rev. Mod. Phys. **79**, 1217 (2007).
[43] Z. H. Xiong, D. Wu, Z. Valy Vardeny, and J. Shi, Nature (London) **427**, 821 (2004).
[44] C. Barraud, P. Seneor, R. Mattana, S. Fusil, K. Bouzehouane, C. Deranlot, P. Graziosi, L. Hueso, I. Bergenti, V. Dediu, F. Petroff, and A. Fert, Nat. Phys. **6**, 615 (2010).
[45] S. Majumdar, R. Laiho, P. Laukkanen, I. J. Väyrynen, H. S. Majumdar, and R. Österbacka, Appl. Phys. Lett. **89**, 122114 (2006).
[46] N. A. Morley, A. Rao, D. Dhandapani, M. R. J. Gibbs, M. Grell, and T. Richardson, J. Appl. Phys. **103**, 07F306 (2008).
[47] P. A. Bobbert, W. Wagemans, F. W. A. van Oost, B. Koopmans, and M. Wohlgenannt, Phys. Rev. Lett. **102**, 156604 (2009).
[48] D. R. McCamey, K. J. van Schooten, W. J. Baker, S.-Y. Lee, S.-Y. Paik, J. M. Lupton, and C. Boehme, Phys. Rev. Lett. **104**, 017601 (2010).
[49] Z. Chen, M. Bird, V. Lemaur, G. Radtke, J. Cornil, M. Heeney, I. McCulloch, and H. Sirringhaus, Phys. Rev. B **84**, 115211 (2011).
[50] A. Weller, F. Nolting, and H. Staerk, Chem. Phys. Lett. **96**, 24 (1983).